PHYSICAL REVIEW A **74**, 061401(R) (2006)

Decoding the state distribution in a nonadiabatic rotational excitation by a nonresonant intense laser field

Hirokazu Hasegawa and Yasuhiro Ohshima*
Institute for Molecular Science, National Institutes of Natural Sciences, Myodaiji, Okazaki 444-8585, Japan
and SOKENDAI (The Graduate University for Advanced Studies), Okazaki 444-8585, Japan
(Received 12 July 2006; published 11 December 2006)

We investigated the quantum-state distribution in nonadiabatic rotational excitation induced by a nonresonant intense laser field. NO molecules, initially prepared in the lowest $J=0.5$ state, were rotationally excited to states with up to $J=8.5$ at a laser intensity of 2.5×10^{13} W/cm^2. The characteristics in the observed state distribution were quantitatively reproduced by a quantum dynamical calculation, and excitation pathways typical to molecules in a doubly degenerate state were identified.

DOI: 10.1103/PhysRevA.74.061401 PACS number(s): 42.50.Hz, 33.20.Lg, 33.20.Sn, 42.50.Md

Nonadiabatic molecular alignment induced by intense short laser pulses has been attracting much attention because of the interesting physics involved and possible broader applications [1]. Here, a rotational wave packet is created from an initial stationary state via an interaction between the molecular anisotropic polarizability and polarized laser fields with much shorter duration than the characteristic time for molecular rotation. Thus, nonadiabatic alignment is inherently accompanied by nonadiabatic rotational excitation (NAREX), which yields novel ensembles of molecules residing in states with higher rotational angular momentum while preserving the azimuthal quantum number as the initial value [2–5].

While most of the previous studies have been devoted to exploring the degree of molecular alignment and its time evolution, by utilizing various real-time measurements [2,3,6–10], the state distribution in NAREX has not been focused on despite of the following physical significances. First, details concerning the excitation process during exposure to laser fields are encoded in the state distribution. Once this information is used complementarily with a real-time evaluation of the molecular alignment, it may lead to a full experimental reconstruction of the rotational density matrix [11]. Second, molecules in highly anisotropic states exerted to NAREX will be particularly useful for studies of, e.g., quantum-state resolved collisional or reaction dynamics. Third, NAREX can become a competent tool for changing and controlling the rotational-state distribution of molecules, especially when recent elaborate methods—i.e., double-pulse pairs [12–14] and shaped pulses [15,16]—are invoked.

In the present work we performed a direct measurement of the rotational-state distribution of a molecule irradiated by a nonresonant femtosecond (fs) laser pulse by utilizing a frequency-domain spectroscopic probe with almost full quantum-state resolution. We give an experimental observation in a state-resolved manner of molecules exposed to intense laser fields beyond the perturbative regime. Nitric oxide (NO) was chosen as a molecule to be examined primarily because of easy access for probing the distribution by resonant-enhanced multiphoton ionization (REMPI) and secondary because of its characteristic rotational energy-level structure in the doubly degenerate electronic ground state. A theoretical calculation was conducted to show a quantitatively good agreement with the experimental results, and an excitation process in NAREX unique to $^2\Pi$ molecules has been unveiled.

In our experiment, a pulsed molecular beam of 0.5% NO diluted in Ne with a stagnation pressure of 2.5 atm was produced in a differentially pumped vacuum chamber. The rotational temperature was adiabatically cooled to less than 2 K, where only states with $J=0.5$ were essentially populated. The molecular beam was then sequentially exposed with two laser fields: a fs Ti:sapphire laser (810 nm, 1 mJ/pulse, 150 fs duration) and the doubled output from a nanosecond (ns) dye laser ($\sim$226 nm, an energy resolution of 0.4 cm^{-1}, 20 μJ/pulse, 10 ns duration) following after 100 ns. Because decreasing the delay down to 50 ns brought about no substantial change in the observed spectra, collisional relaxation was negligible. Here, we refer to the former fs pulse as the pump and the latter ns pulse as the probe, respectively. The pump pulse was focused by a lens of $f=300$ mm on the molecular beam. The $A\,^2\Sigma^+\leftarrow X\,^2\Pi_{1/2}$ (0–0) band of NO was recorded by (1+1) REMPI by scanning the probe laser frequency. A lens of $f=170$ mm was used for focusing the probe pulse and the pump pulse was slightly defocused from the interaction region by $\sim$5 mm to maximize the laser-beam overlap. The focal spot diameters were estimated to be 150 μm for the pump and 30 μm for the probe. NO^+ ions thus generated by REMPI were detected by a linear time-of-flight (TOF) mass spectrometer. Both polarizations of the fs pump and the ns probe lasers were set parallel to the ion-extraction field.

Figure 1 shows the (1+1) REMPI excitation spectra of the $A\,^2\Sigma^+\leftarrow X\,^2\Pi_{1/2}$ (0–0) band recorded at various pump pulse energies. As shown in panel (a), the spectrum measured without the pump pulse exhibits only three lines in the Q_{11}, $Q_{21}+R_{11}$, and R_{21} branches with a common lower state of $J=0.5$. This observation ensures that the initial distribution is restricted to the single lowest state due to efficient rotational cooling. Panels (b), (c), and (d) correspond to the spectra measured with pump energies of 0.17, 0.35, and 0.62 mJ, respectively. The new spectral lines appear when a pump field is applied. Transitions from states with the maxi-

*Electronic address: ohshima@ims.ac.jp

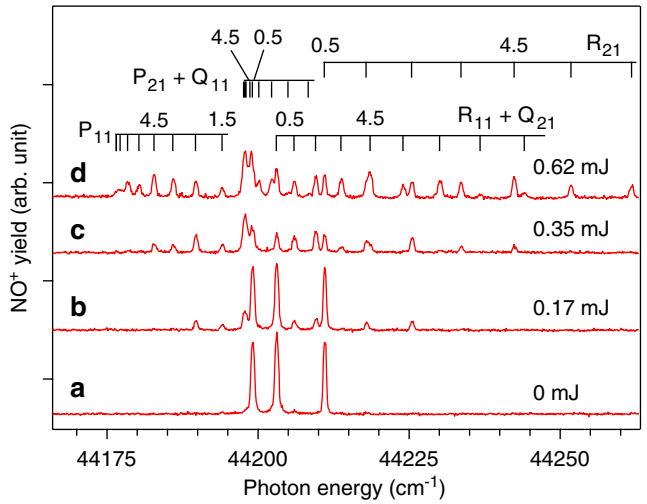

FIG. 1. (Color online) (1+1) REMPI excitation spectra of the $A\,^2\Sigma^+ \leftarrow X\,^2\Pi_{1/2}$ (0–0) band of NO. Spectra (a)–(d) were measured by using pump energies of 0, 0.17, 0.35, and 0.62 mJ, respectively. The assignments of the lines are also displayed at the top of the figure.

mum J up to 2.5, 4.5, and 8.5 were observed for the applied pump energies. By dividing the observed intensities by the transition probabilities for each rotational line in the A–X transition, the rotational-state distribution of pumped NO molecules in $X\,^2\Pi_{1/2}$ was derived, as shown in Fig. 2. Here, the plotted values for each J are the average from three transitions in the R_{21}, $R_{11}+Q_{21}$, and P_{11} branches with the common lower J, while lines in $P_{21}+Q_{11}$ were not included because overlapping lines. The indicated errors correspond to one standard deviation for data from the three different types of transitions.

It is evident in Fig. 2 that the rotational-state distribution is spread among a wider range of J from the initial distribution confined to the single $J=0.5$ state and its peak shifts to higher J values as the pump laser intensity is increased. More remarkably, the state distribution observed in NO($X\,^2\Pi_{1/2}$) *does not* vary smoothly against J. For instance, states with

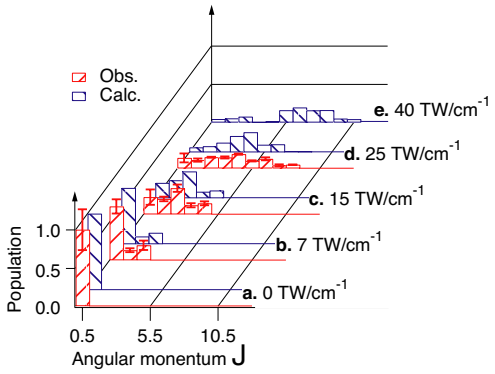

FIG. 2. (Color online) Observed and calculated rotational-state distributions of NO pumped by fs laser intensities of (a) 0 TW/cm^2 (0 mJ), (b) 7 TW/cm^2 (0.17 mJ), (c) 15 TW/cm^2 (0.35 mJ), (d) 25 TW/cm^2 (0.62 mJ), and (e) 40 TW/cm^2. The values in parentheses are the corresponding experimental pump pulse energies.

$J=2.5$, 4.5, and 6.5 have a larger population than the adjacent $J=1.5$, 3.5, and 5.5 states. Such a kind of variation in the distribution from a single initial state has not been observed in the case of molecules in a nondegenerate electronic state—e.g., N_2 ($X\,^1\Sigma_g^+$) [5]. In order to explain this feature and to investigate the nonadiabatic rotational-excitation process, the time-dependent Schrödinger equation was solved numerically.

The interaction of a molecular anisotropic polarizability with a linearly polarized nonresonant laser field can be expressed by $\hat{V}=-\frac{1}{4}[E(t)]^2(\Delta\alpha\cos^2\theta+\alpha_\perp)$, where $E(t)$ is the envelope of the electric field of the laser pulse, $\Delta\alpha=\alpha_\parallel-\alpha_\perp$, with static polarizabilities parallel and perpendicular to the molecular axis, $\alpha_\parallel$ and $\alpha_\perp$, respectively, and θ is the angle between the molecular axis and the laser polarization [17]. The time-dependent rotational wave function of NO can be expanded by Hund's case (a) basis set [18], $|X\,^2\Pi_{1/2};J,\Omega,M,p\rangle$, for field-free rotation, as $|\Psi(t);M,p\rangle=\Sigma_J^\infty d_{JMp}(t)e^{-iE_Jt/\hbar}|X\,^2\Pi_{1/2};J,\Omega,M,p\rangle$, where p represents the $\pm$ parity of the state, $d_{JMp}(t)$ is the probability amplitude, and $E_J=B(J+1/2)^2$ is the rotational energy of the $|X\,^2\Pi_{1/2};J,\Omega,M,p\rangle$ state with B as the rotational constant. Because the total Hamiltonian is invariant to inversion in space, $|\Psi(t);M,p\rangle$ has definite parity and is composed of bases with the same parity. In addition, because we consider here the linearly polarized laser field, M is also preserved. Consequently, the time-dependent Schrödinger equation can been converted to coupled equations on $d_{JMp}(t)$ [3,5], in which the interaction matrix element is explicitly expressed by

$$V_{JJ'}^{Mp} \equiv \langle X\,^2\Pi_{1/2};J,\Omega,M,p|\hat{V}|X\,^2\Pi_{1/2};J',\Omega,M,p\rangle$$
$$= -\frac{1}{4}[E(t)]^2\left\{\frac{2}{3}\Delta\alpha(-1)^{M-1/2}\sqrt{(2J+1)(2J'+1)}\right.$$
$$\left.\times\begin{pmatrix} J & 2 & J' \\ -M & 0 & M \end{pmatrix}\begin{pmatrix} J & 2 & J' \\ -\Omega & 0 & \Omega \end{pmatrix}-\left(\frac{1}{3}\Delta\alpha+\alpha_\perp\right)\delta_{J,J'}\right\}. \quad (1)$$

Because the value of $V_{JJ'}^{Mp}$ is the same for $p=+$ and $-$, the resultant time-dependent wave functions with different parities (and d_{JMp} accordingly) are identical to each other. The coupled equations were numerically solved under the initial condition of $J=0.5$ and $M=0.5$. We used a rotational constant of $B=1.696$ cm^{-1} [19] and volume polarizabilities of $\alpha_\parallel=2.26$ Å^3 and $\alpha_\perp=1.43$ Å^3 [20]. The static polarizabilities can be obtained by $\alpha_{\text{static}}=4\pi\epsilon_0\alpha_{\text{volume}}$, where ϵ_0 is the permittivity of a vacuum. $[E(t)]^2$ was assumed to have as a Gaussian shape with a full width at half maximum of 150 fs. As shown in Fig. 2, the observed rotational-state distributions at 0.17, 0.35, and 0.62 mJ agree well with the calculated ones having laser intensities of 7, 15, and 25 TW/cm^2. When we evaluated the intensity from the total laser power and the estimated laser spot size at the focal point, the values were overestimated by 3 times. This overestimation should be due to a slight misalignment between the two laser beams

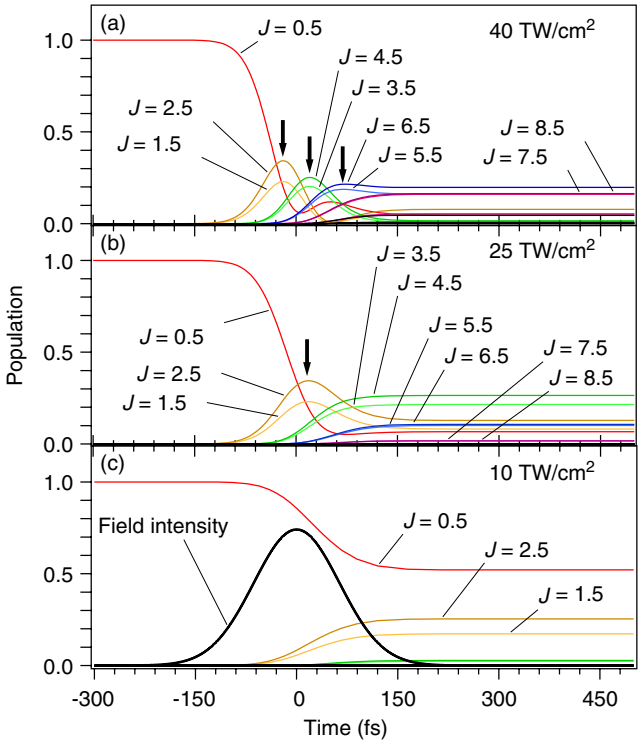

FIG. 3. (Color online) Time evolution of the rotational-state distribution calculated at pump intensities of (a) 7 TW/cm^2, (b) 25 TW/cm^2, and (c) 40 TW/cm^2. The peaks of the pairing states are shown by arrows in (b) and (c).

and/or an uncertainty in the estimated spot size caused by astigmatism.

The time evolution of the probability densities, $|d_{JMp}(t)|^2$, of NO irradiated by a fs laser pulse with various laser intensities is shown in Fig. 3. The figures show a stepwise evolution from the initial state to higher-J states, which is induced by the Raman-type excitation process governed by the $\hat{V}$ interaction. Even though each excitation only involves changes in J by 1 or 2, because of the nonvanishing matrix elements in Eq. (1), such excitations can proceed successively to transfer the population from low-J to higher-J states until the laser field diminishes. As the laser intensity is increased, the buildup (and the subsequent falloff) of rotational populations for each states becomes faster and, as a consequence, excitation to higher-J states is achieved.

A similar stepwise evolution of the rotational population has already been reported in the calculation for N_2 [5]. A notable difference in the case of NO is the existence of excitation pathways of $\Delta J=1$ in addition to $\Delta J=2$, which allows all of the rotational states to be coupled with the initial $J=0.5$ state. On the other hand, only $\Delta J=2$ pathways are allowed, for N_2; states with even (or odd) J can only be excited from the initial state with $J=0$ (or 1). This difference originates from the unquenched electronic angular momentum Ω for NO in the $X\,^2\Pi$ state, where each rotational state with a certain J is composed of a doubly degenerate Λ-doubling pair with $+$ and $-$ parities. Therefore, $\Delta J=1$ coupling is allowed by the $\hat{V}$ interaction, which couples states with the same parity. In contrast, because an adjacent rotational state has a different parity for molecules with $\Omega=0$, such as N_2 ($X\,^1\Sigma_g^+$) [3,9,5], CO ($X\,^1\Sigma^+$) [8], and O_2 ($X\,^3\Sigma_u^-$) [3,9,10], $\Delta J=1$ coupling is forbidden for them. It is noted that linear molecules in vibrationally excited states of degenerate bending modes or symmetric-top molecules in states with $K\neq 0$ will behave like NO in $X\,^2\Pi$.

A detailed examination of Fig. 3 reveals a characteristic phenomenon in the rotational-state evolution in NO ($X\,^2\Pi_{1/2}$): pairs of adjacent states ({1.5, 2.5}, {3.5, 4.5}, {5.5, 6.5} and so on) show an almost identical time dependence, and the population of 1.5 (3.5, 5.5, …) is smaller than that of 2.5 (4.5, 6.5, …). This fact is explained as follows: because $\Delta J=1$ and 2 couplings are allowed, the initial population of $J=0.5$ is transferred to states with $J=1.5$ and 2.5 almost simultaneously in the first excitation step. Subsequent excitations with $\Delta J=1$ and 2 further transfer the population to higher J states in a stepwise manner. However, the coupling strengths given in Eq. (1) become dominant for $\Delta J=2$ over those for $\Delta J=1$ as J increases. Therefore, most of the population from $J=1.5$ is transferred to $J=3.5$, while $J=2.5$–4.5. As a result, the state population is nonadiabatically transferred via two separate excitation pathways, starting from the common initial state, $J=0.5\rightarrow 1.5\rightarrow 3.5\rightarrow 5.5\rightarrow\cdots$ and $J=0.5\rightarrow 2.5\rightarrow 4.5\rightarrow 6.5\rightarrow\cdots$. Because the population transferred in the first step is smaller in the former pathway, the subsequent states also have a smaller population than those in the latter pathway. The existence of the two distinct excitation pathways directly causes the previously mentioned dominating population for 2.5, 4.5, … in the observed state distribution of NO ($X\,^2\Pi_{1/2}$).

The present experimental determination of the rotational-state distribution in NAREX opens up multiple applications in intense-laser physics and the control of molecular processes. First, the method should be utilized for detailed investigations of the excitation processes of various molecular systems. Systems of particular interest are asymmetric-top molecules, in which the multidimensional character has been subjected to substantial theoretical and experimental studies [6]. Another fascinating problem to be explored is the excitation mechanism in an "optical centrifuge"[21], where chirped pulses with rotating polarization have been used to accelerate molecular rotation, so that the molecule dissociates. Second, the method can be extended to manipulate the rotational-state distribution by controlled NAREX. For instance, excitation with a single pump pulse may not go beyond the maximum J over 10.5 in the case of NO, for which multiple ionization by enhanced ionization [22,23] becomes prominent at 40 TW/cm^2 [24]. The limit will be overcome by implementation of multiple-pulse excitation or pulse shaping, which has been shown to be efficient for enhancing transient spatial alignment [12,15,16,25]. Double-pulse excitation has also been used for the phase control of rotational wave packets [14]. In this study, a second pulse was introduced at fractional revivals to interfere two wave packets. Such interference will be traced in the state distribution, and it will be particularly interesting to examine the "zero-pulse" pair, which annihilates the wave packet created by the first pulse and returns the molecular ensemble back to the initial state [14].

In summary, we have demonstrated quantum-state resolved observations in nonadiabatic rotational population transfer by a nonresonant intense laser field. We employed jet-cooled NO molecules, of which all of the population was confined to the lowest $J=0.5$ state and the molecular ensemble was irradiated by a strong 810-nm laser pulse with 150 fs duration. The resultant rotational-state distribution after nonadiabatic rotational excitation was investigated by (1+1) REMPI detection employing a ns laser probe with almost full rotational resolution, and a variation of the state distribution against the laser field intensity up to 25 TW/cm^2 was systematically examined. A quantum dynamical calculation, appropriated to $^2\Pi$ molecules, like NO, was conducted to reveal the characteristic pairing of adjacent states in the time evolution of the population. This trend, due to the existence of two distinct excitation pathways, governed the final-state distribution, as observed here.

The authors thank Professor Akiyoshi Hishikawa for providing the NO sample. This work was partly supported by Grants-in-Aid from MEXT Japan (Nos. 15035206, 16032206, 18244120, and 18750020) and the RIKEN-IMS joint program on "Extreme Photonics." Additional financial support from the Research Foundation for Opto-Science and Technology and the Mitsubishi Foundation is also appreciated.

[1] H. Stapelfeldt and T. Seideman, Rev. Mod. Phys. **75**, 543 (2003).
[2] F. Rosca-Pruna and M. J. J. Vrakking, Phys. Rev. Lett. **87**, 153902 (2001); J. Chem. Phys. **116**, 6567 (2002); **116**, 6579 (2002).
[3] P. W. Dooley, I. V. Litvinyuk, K. F. Lee, D. M. Rayner, M. Spanner, D. M. Villeneuve, and P. B. Corkum, Phys. Rev. A **68**, 023406 (2003).
[4] J. Ortigoso, M. Rodríguez, M. Gupta, and B. Friedrich, J. Chem. Phys. **110**, 3870 (1999).
[5] M. Tsubouchi and T. Suzuki, Phys. Rev. A **72**, 022512 (2005).
[6] E. Péronne, M. D. Poulsen, C. Z. Bisgaard, H. Stapelfeldt, and T. Seideman, Phys. Rev. Lett. **91**, 043003 (2003); M. D. Poulsen, E. Péronne, H. Stapelfeldt, C. Z. Bisgaard, S. S. Viftrup, E. Hamilton, and T. Seideman, J. Chem. Phys. **121**, 783 (2004).
[7] V. Renard, M. Renard, S. Guérin, Y. T. Pashayan, B. Lavorel, O. Faucher, and H. R. Jauslin, Phys. Rev. Lett. **90**, 153601 (2003).
[8] D. Pinkham and R. R. Jones, Phys. Rev. A **72**, 023418 (2005).
[9] K. Miyazaki, M. Kaku, G. Miyaji, A. Abdurrouf, and F. H. M. Faisal, Phys. Rev. Lett. **95**, 243903 (2005).
[10] V. G. Stavros, E. Harel, and S. R. Leone, J. Chem. Phys. **122**, 064301 (2005).
[11] A. S. Mouritzen and K. Mølmer, J. Chem. Phys. **124**, 244311 (2006).
[12] C. Z. Bisgaard, M. D. Poulsen, E. Péronne, S. S. Viftrup, and H. Stapelfeldt, Phys. Rev. Lett. **92**, 173004 (2004); C. Z. Bisgaard, S. S. Viftrup, and H. Stapelfeldt, Phys. Rev. A **73**, 053410 (2006).
[13] K. F. Lee, I. V. Litvinyuk, P. W. Dooley, M. Spanner, D. M. Villeneuve, and P. B. Corkum, J. Phys. B **37**, L43 (2004).
[14] K. F. Lee, D. M. Villeneuve, P. B. Corkum, and E. A. Shapiro, Phys. Rev. Lett. **93**, 233601 (2004); K. F. Lee, E. A. Shapiro, D. M. Villeneuve, and P. B. Corkum, Phys. Rev. A **73**, 033403 (2006).
[15] M. Renard, E. Hertz, S. Guérin, H. R. Jauslin, B. Lavorel, and O. Faucher, Phys. Rev. A **72**, 025401 (2005).
[16] C. Horn, M. Wollenhaupt, M. Krug, T. Baumert, R. de Nalda, and L. Bañares, Phys. Rev. A **73**, 031401(R) (2006).
[17] B. Friedrich and D. Herschbach, Phys. Rev. Lett. **74**, 4623 (1995).
[18] R. N. Zare, *Angular Momentum* (Wiley-Interscience, New York, 1988).
[19] J. Danielak, U. Domin, R. Kępa, M. Rytel, and M. Zachwieja, J. Mol. Spectrosc. **181**, 394 (1997).
[20] P. Bundgen, A. J. Thakkar, A. Kumar, and W. J. Meath, Mol. Phys. **90**, 721 (1997); S. A. C. McDowell and W. J. Meath, Can. J. Phys. **76**, 483 (1998).
[21] D. M. Villeneuve, S. A. Aseyev, P. Dietrich, M. Spanner, M. Yu. Ivanov, and P. B. Corkum, Phys. Rev. Lett. **85**, 542 (2000).
[22] J. H. Posthumus, L. J. Frasinski, A. J. Giles, and K. Codling, J. Phys. B **28**, L349 (1995).
[23] T. Seideman, M. Y. Ivanov, and P. B. Corkum, Phys. Rev. Lett. **75**, 2819 (1995).
[24] A. Talebpour, S. Larochelle, and S. L. Chin, J. Phys. B **30**, L245 (1997).
[25] M. Leibscher, I. Sh. Averbukh, and H. Rabitz, Phys. Rev. Lett. **90**, 213001 (2003).